



Analysis of autocatalytic networks in biology[☆]

Gentian Buzi^{*}, Ufuk Topcu, John C. Doyle

Control and Dynamical Systems, California Institute of Technology, Pasadena, CA 91125, USA

ARTICLE INFO

Article history:

Received 1 February 2010

Received in revised form

21 January 2011

Accepted 2 February 2011

Available online 21 March 2011

Keywords:

Autocatalytic pathways

Glycolysis

Quantitative analysis

Compositional analysis

Nonlinear systems

ABSTRACT

Autocatalytic networks, in particular the glycolytic pathway, constitute an important part of the cell metabolism. Changes in the concentration of metabolites and catalyzing enzymes during the lifetime of the cell can lead to perturbations from its nominal operating condition. We investigate the effects of such perturbations on stability properties, e.g., the extent of regions of attraction, of a particular family of autocatalytic network models. Numerical experiments demonstrate that systems that are robust with respect to perturbations in the parameter space have an easily “verifiable” (in terms of proof complexity) region of attraction properties. Motivated by the computational complexity of optimization-based formulations, we take a compositional approach and exploit a natural decomposition of the system, induced by the underlying biological structure, into a feedback interconnection of two input–output subsystems: a small subsystem with complicating nonlinearities and a large subsystem with simple dynamics. This decomposition simplifies the analysis of large pathways by assembling region of attraction certificates based on the input–output properties of the subsystems. It enables numerical as well as analytical construction of block-diagonal Lyapunov functions for a large family of autocatalytic pathways.

© 2011 Elsevier Ltd. All rights reserved.

1. Introduction

Core metabolism in cells is comprised of metabolic reaction networks (pathways), which are sequences of chemical reactions usually connected in series, catalyzed by enzymes. These enzymes regulate (control) the metabolic pathways via two distinct mechanisms: transcriptional regulation on a slow time-scale and allosteric regulation on a fast time-scale (Alberts et al., 2002). Some metabolic pathways contain reactions that require the consumption of one of their own products, thus creating a positive feedback loop. Such pathways are called autocatalytic pathways. They are very common in biology; indeed, at a certain level, all biological networks are autocatalytic, since, in every cell, food and resources are broken down to create energy and components via processes that also require the use of those same components and energy. One such pathway is the glycolysis pathway, which the cell relies on to produce energy anaerobically by breaking down glucose. This pathway produces four ATP molecules (energy

carriers) while consuming two ATP molecules early in the pathway (i.e., autocatalysis). One of the catalyzing enzymes, PFK, is allosterically regulated by ATP: PFK is inhibited when ATP concentration is high (Banuelos, Gancedo, & Gancedo, 1977).

Biochemical networks with different topologies and different reaction rate constraints have been subject to study for many decades. Results regarding the number of and convergence properties around steady states for certain rather general networks with mass-action kinetics are established in Feinberg (1988), Feinberg (1995), and Horn and Jackson (1972). The theory of monotone dynamical systems (Sontag, 2007) has proven to be a powerful tool for understanding the behavior of biological systems. Using this theory, certain network topologies are shown to have global convergence for quite general reaction rates (de Leenheer, Angeli, & Sontag, 2007). A sufficient stability criterion (for linearized dynamics) is established for cyclic interconnection networks with inhibition of the first reaction by the end product (Thron, 1991; Tyson & Othmer, 1978). These results are extended to prove global asymptotic stability using passivity of subsystems under certain conditions on the reaction rates (Arcak & Sontag, 2006, 2008).

In this paper, we study metabolic networks with the topology in Fig. 1. In general, these networks do not exhibit global convergence properties, and they can have multiple equilibrium points, each with a large region of attraction (RoA). Many of the interesting properties of these networks are induced by the interplay of autocatalysis and negative allosteric regulation. Changes in metabolite and catalyzing enzyme concentrations during the lifetime of the cell can perturb the system from the nominal operating point. We investigate robustness to such perturbations through

[☆] This work was supported by the NIH (award# R01 GM078992A), the Institute of Collaborative Biotechnologies from the U.S. Army Research Office (UCSB award# KK9150, ARO prime award# W911NF-09-D-0001), and AFOSR (FA9550-08-1-0043). The material in this paper was partially presented at the 2010 American Control Conference, June 30–July 2, 2010, Baltimore, Maryland, USA. This paper was recommended for publication in revised form by Associate Editor Elling Jacobsen under the direction of Editor Frank Allgöwer.

^{*} Corresponding author. Tel.: +1 626 755 7837; fax: +1 626 395 6170.

E-mail addresses: genti@cds.caltech.edu (G. Buzi), utopcu@cds.caltech.edu (U. Topcu), doyle@cds.caltech.edu (J.C. Doyle).

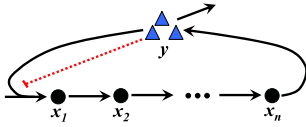
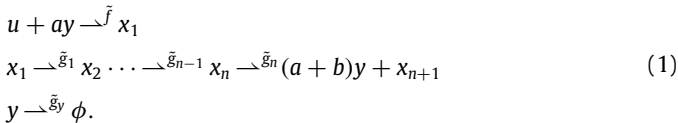


Fig. 1. A schematic of an autocatalytic pathway with feedback inhibition. The final pathway product y (blue triangles) is consumed to convert the input of the pathway into the first metabolite x_1 . Additionally, y inhibits (dotted red line) the enzyme that catalyzes the autocatalytic reaction.

optimization-based estimation of the RoA (a measure of the extent of perturbations from which the system recovers) around nominal operating conditions (Khalil, 2002). The resulting numerical procedure is effective on relatively small pathways and becomes challenging for large pathways due to computational complexity. We partially alleviate this computational burden by exploiting the underlying biological structure, which offers a natural decomposition of the system into a feedback interconnection of two input–output subsystems: a small subsystem with “complicating” nonlinearities and a large subsystem with simple dynamics. This decomposition enables compositional RoA analysis based on the input–output properties of the subsystems. It enables numerical construction of block-diagonal Lyapunov functions, which provide algebraic characterizations of invariant subsets of the RoA, for families of pathways that are not amenable to direct analysis. Furthermore, it leads to analytical construction of Lyapunov functions for a large family of autocatalytic pathways.

2. An autocatalytic pathway model

Consider the autocatalytic metabolic pathway with multiple intermediate metabolite reactions (see Fig. 1)



Here, u is some precursor and source of energy for the pathway with no dynamics associated, y denotes the product of the pathway, x_i are intermediate metabolites, ϕ is a null state, a is the number of y molecules that are invested in the pathway, and $a+b$ is the number of y molecules produced. $A \xrightarrow{f} B$ denotes a chemical reaction that converts the chemical species A to the chemical species B at rate f . Then, a set of ordinary differential equations that govern the changes in concentrations x_1, \dots, x_n , and y can be written as

$$\begin{aligned} \dot{x}_1 &= \tilde{f}(y) - \tilde{g}_1(x_1) \\ \dot{x}_i &= \tilde{g}_{i-1}(x_{i-1}) - \tilde{g}_i(x_i), \quad \text{for } i = 2, \dots, n \\ \dot{y} &= (a+b)\tilde{g}_n(x_n) - a\tilde{f}(y) - \tilde{g}_y(y), \end{aligned} \quad (2)$$

for $x_i \geq 0, y \geq 0$. Here, $\tilde{g}_1, \dots, \tilde{g}_n$, and \tilde{g}_y are continuous, monotone, increasing functions that vanish at 0 (consistent with large classes of chemical kinetics models such as mass-action and Michaelis–Menten). We choose $\tilde{f}(y) = \frac{V\gamma^q}{1+\gamma y^h}$, which is consistent with biological intuition and experimental data in the case of the glycolysis pathway (Banelos et al., 1977; Dano, Madsen, Schmidt, & Cedersund, 2006), where $V > 0$ depends on u (pathway input), $q > 0$ captures the strength of autocatalysis, and $\gamma, h > 0$ capture the strength of inhibition. Note that \tilde{f} is not monotone and captures the interplay between the autocatalysis and inhibition. For the rest of the paper, we take $a = b = 1$ and note that the results generalize straightforwardly for $a, b > 0$.

The pathway in (1) qualitatively captures the essence of glycolytic oscillations and is similar to many reduced-order

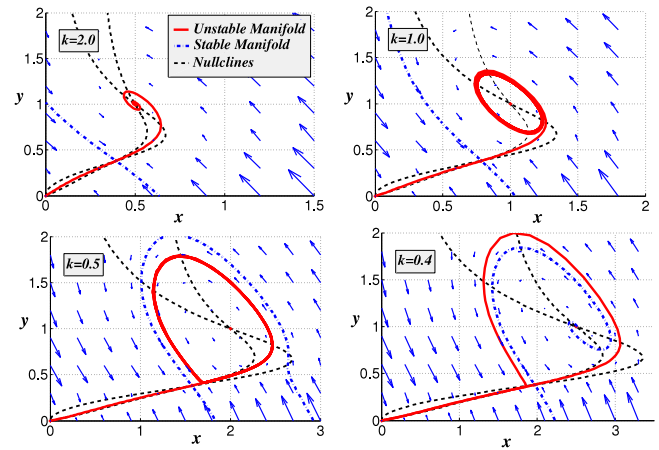


Fig. 2. Changes in the dynamic behavior due to changes in the reaction rate constant k with $n = 1, h = 4, \gamma = 5, q = 2, V = 6, \tilde{g}_y(y) = 1.2y/(0.2 + y)$ and $\tilde{g}_1(x_1) = kx_1$.

glycolysis models in the literature. For example, Dano et al. (2006) reduces the full-scale glycolysis pathway of Hynne, Dano, and Sorensen (2001) to models with eight states and then three states, both of them matching well the structure of (1). Eliminating the fast reaction from the three-state model results in the two-state model of Chandra, Buzi, and Doyle (2009), which is identical to (1) for $n = 1$. The purpose of using the particular model family in (1) is twofold: to get insights into how to analyze such models in general and to get a deeper understanding of tradeoffs that biology faces. To this end, the model has been selected to be more homogeneous and structured than real biology (such as ignoring the specific features of each enzyme and metabolite), so that both quantitative analysis tools and models of different order can be compared.

Under perturbations in the reaction rates (e.g., as a result of changes in enzyme concentrations), system (2) can exhibit a rich dynamic behavior including oscillations observed in glycolysis and glycolysis models in the literature (Nielsen & Sorensen, 1998; Richard, 2003). Fig. 2 illustrates such changes in behavior for a model pathway as the system goes through Hopf and homoclinic bifurcations due to changes in k . Additionally, the equilibrium concentrations of the intermediate metabolites depend on the concentration of the catalyzing enzymes. Sudden drops in the corresponding enzyme concentrations will cause perturbations in the concentrations of the intermediate metabolites. How big can this drop be if the system is to converge to the new equilibrium rather than have all concentrations converging to zero and the cell dying? In the following, we show that estimation of the region of attraction around a nominal operating condition for (2) can be used to study such questions.

3. Region of attraction analysis

3.1. Estimation of the region of attraction

Consider the system governed by

$$\dot{\xi}(t) = F(\xi(t)), \quad (3)$$

where $\xi(t) \in \mathcal{R}^m$ is the state vector and $F : \mathbb{R}^m \rightarrow \mathbb{R}^m$ is such that $F(0) = 0$, i.e., the origin is an equilibrium point of (3) and F is locally Lipschitz on \mathbb{R}^m . Let $\varphi(t, \xi)$ denote the solution to (3) with the initial condition $\varphi(0, \xi) = \xi$ at time t . The region of attraction (RoA) of the origin for (3) is $\{\xi \in \mathbb{R}^m : \lim_{t \rightarrow \infty} \varphi(t, \xi) = 0\}$. For $\eta > 0$ and a function $U : \mathbb{R}^m \rightarrow \mathbb{R}$, define the η -sublevel set of U as $\Omega_{U, \eta} := \{\xi \in \mathbb{R}^m : U(\xi) \leq \eta\}$. We use the following characterization of the invariant subsets of the RoA.

Lemma 1 (Topcu, Packard, & Seiler, 2008). Let $\alpha > 0$. If there exists a continuously differentiable function $U : \mathbb{R}^m \rightarrow \mathbb{R}$ such that

$$\Omega_{U,\alpha} \text{ is bounded,} \tag{4}$$

$$U(0) = 0, \quad U(\xi) > 0 \text{ for all } \xi \neq 0, \text{ and} \tag{5}$$

$$\Omega_{U,\alpha} \setminus \{0\} \subset \{\xi \in \mathbb{R}^m : \nabla U(\xi)F(\xi) < 0\}, \tag{6}$$

then $\Omega_{U,\alpha}$ is invariant and in the RoA of the origin for (3).

When F is a vector of polynomials, the search for polynomial Lyapunov functions U that characterize invariant subsets of the RoA through Lemma 1 can be performed as a sum-of-squares (SOS) optimization problem (Parrilo, 2003). For example, the optimal values of U^* , α^* , and β^* of U , α , and β , respectively, in the optimization

$$\begin{aligned} & \max_{U \in \mathcal{U}, \alpha, \beta > 0, s_i \in \mathcal{S}_i} \beta \quad \text{subject to} \\ & U(0) = 0, \quad U - l_1, s_1, s_2, \text{ and } s_3 \text{ are SOS,} \\ & -[(\beta - \xi^T \xi)s_1 + (U - \alpha)] \text{ is SOS,} \\ & -[(\alpha - U)s_2 + \nabla U F s_3 + l_2] \text{ is SOS} \end{aligned} \tag{7}$$

satisfy $\{\xi \in \mathbb{R}^m : \xi^T \xi \leq \beta^*\} \subset \Omega_{U^*, \alpha^*}$, and Ω_{U^*, α^*} is contained in the RoA. In (7), l_1 and l_2 are positive-definite polynomials, and the sets \mathcal{U} , \mathcal{S}_1 , \mathcal{S}_2 , and \mathcal{S}_3 are prescribed finite-dimensional subspaces of polynomials. The optimization in (7) is a bilinear semidefinite program and may be nonconvex. Topcu et al. (2008) and Topcu, Packard, Seiler, and Balas (2010) discuss strategies for computing suboptimal solutions for this problem.

3.2. Application to the autocatalytic network model

Let $\bar{\xi} = [\bar{x}_1, \dots, \bar{x}_n, \bar{y}]^T$ be a fixed point of (2) (the operating condition of interest) in the (strictly) positive orthant. Without loss of generality, we use the normalization $\bar{y} = 1$, which implies that $V = r_y(1 + \gamma)$ with $r_y := \bar{g}_y(\bar{y})$. A change of coordinates to move the fixed point $\bar{\xi}$ to the origin enables us, with some abuse of notation, to write the vector field as

$$\begin{aligned} \dot{x}_1 &= f(y) - g_1(x_1) \\ \dot{x}_i &= g_{i-1}(x_{i-1}) - g_i(x_i), \quad \text{for } i = 2, \dots, n \\ \dot{y} &= 2g_n(x_n) - f(y) - g_y(y) \end{aligned} \tag{8}$$

in $\mathcal{D} := \{\xi \in \mathbb{R}^{n+1} : \xi_i \geq -\bar{\xi}_i, i = 1, \dots, n + 1\}$, where $f(y) = \frac{r_y(1+\gamma)(y+1)^q}{1+\gamma(y+1)^h} - r_y$. Note that g_1, \dots, g_n , and g_y are continuous, monotone, increasing, and vanish at 0.

Optimization (7) provides a means for computing invariant subsets of the RoA for systems with polynomial vector fields. When g_1, \dots, g_n, g_y are polynomials and q and h are integers, the vector field in (8) is rational, and straightforward generalizations of the conditions in (7), obtained through Lemma 2, can be used. To this end, rewrite the vector field in (8) as $G(\xi)/H(y)$, where $H(y) := 1 + \gamma(y + 1)^h$ and G is a vector of polynomials in ξ . Note that $H(y) > 0$ for all $y \geq -1$ and $G(0) = 0$. Then, the following can be proven using the invariance of \mathcal{D} under the flow of (8) and Lemma 1.

Lemma 2. Let U be a continuously differentiable function, $\alpha > 0$, and U, α satisfying the conditions in (4)–(5) and $\Omega_{U,\alpha} \setminus \{0\} \subset \{\xi \in \mathbb{R}^{n+1} : \nabla U(\xi)G(\xi) < 0\}$. Then, $\Omega_{U,\alpha} \cap \mathcal{D}$ is invariant and is contained in the RoA of the origin for (8).

For the rest of this section, we assume $g_1(x_1) = k_1 x_1, \dots, g_n(x_n) = k_n x_n, g_y(y) = k_y y$, and q and h to be positive integers. For ease of exposition, we set $q = 1, k_1 = \dots = k_n = k$, scale the time so that $k_y = 1$, and investigate the robustness of the system (8) in terms of the extent of the quantified RoA estimates around the origin using the following measures.

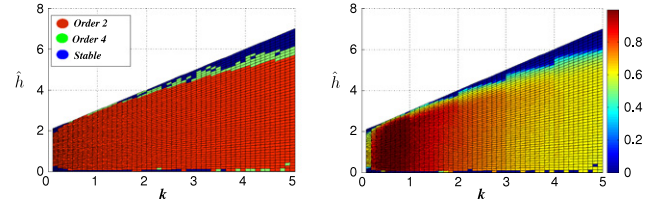


Fig. 3. Left: the region marked by red corresponds to the set of parameters for which a quadratic Lyapunov function verifies that $\mathcal{B}_{1/2,k,1}$ is in the RoA, the region marked by green corresponds to the set that needed a quartic Lyapunov function, and the region marked by blue corresponds to linearly asymptotically stable systems for which (7) does not yield an RoA estimate for quadratic or quartic Lyapunov functions. Right: the color bar represents the values of $r^*/\sqrt{1 + 1/k^2}$ for stabilizing values of k and \hat{h} . (For interpretation of the references to colour in this figure legend, the reader is referred to the web version of this article.)

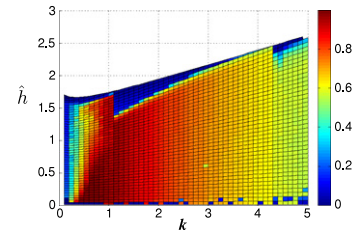


Fig. 4. The color bar represents the values of $r^*/\sqrt{1 + n/k^2}$ for $n = 3$ and for stabilizing values of k and \hat{h} .

- For given $0 < \eta < 1$ and k , the first measure is the *degree of the smallest degree polynomial Lyapunov function* that certifies the set $\mathcal{B}_{\eta,k,n} := \{\xi : \xi^T \xi < \eta^2 (1 + \frac{n}{k^2})\}$ to be in the RoA. Note that $\sqrt{1 + n/k^2}$ is the distance to the nearest fixed point $[-1/k, \dots, -1/k, -1]^T$ to the origin.
- For Lyapunov function candidates of a fixed degree, the second measure is the *maximum value r^* of r* such that the ball $\mathcal{B}(r) := \{\xi : \xi^T \xi < r^2\}$ is certified to be in the RoA through (7).

Next, we define the parameter $\hat{h} := \frac{\gamma}{\gamma+1}h$ that captures the strength of feedback in the linearization of (8) (see Section 4.1 and Chandra et al., 2009). For given k , define \hat{h}_k to be the largest value of \hat{h} such that the system corresponding to (k, \hat{h}) is stable. Consider a grid generated by uniformly picking 50 values of k in $[0, 1, 5]$ and, for each fixed value of k , picking 50 values for \hat{h} in $[0, \hat{h}_k]$.¹ For $n = 1$, Fig. 3 (left) shows that systems away from the stability boundary in the parameter space only require a quadratic Lyapunov function to verify that $\mathcal{B}_{1/2,k,1}$ is in the RoA, while polynomials of higher degree are needed for many of the systems near the boundary. From Fig. 3 (right), the main observation is that as the feedback gain \hat{h} increases and approaches its Hopf bifurcation value, the normalized “radius” $r^*/\sqrt{1 + 1/k^2}$ of the verified RoA gets smaller. Similar interpretations hold for $n = 2$ and 3, illustrated in Fig. 4 for $n = 3$.

The size of the optimization (7) (e.g., the number of decision variables) grows with the length of the pathway (i.e., number of states), the degree of the numerator and denominator of f (i.e., q and h), and the degree of the Lyapunov function candidates. This growth may render the analysis based on SOS programming impractical for even modest length pathways (see Topcu & Packard, 2009 for a more detailed discussion). For larger models, we propose a compositional analysis methodology which exploits the underlying structure of the pathway.

¹ For given k, h is set to the smallest integer greater than or equal to \hat{h}_k , to ensure that the vector field is rational.

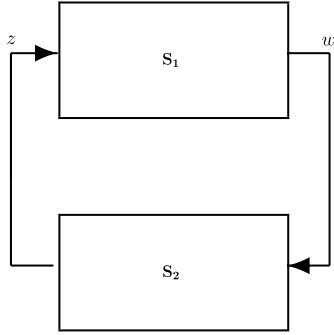


Fig. 5. The system (8) is represented as feedback interconnection of two subsystems S_1 and S_2 .

4. Compositional analysis

We discuss a compositional RoA analysis method using a decomposition of system (8) in Section 4.2, its applications with two different supply rates in Sections 4.3 and 4.4, and its limitations in Section 4.5. We now motivate a notion of local feedback gain for (8) and establish the linear stability bounds used in the rest of the paper.

4.1. Linear stability analysis

Define $k_i := \frac{\partial g_i}{\partial x_i}(0)$, $k_y := \frac{\partial g_y}{\partial y}(0)$. Let $J_{\hat{h}}$ be the Jacobian of (8) around the origin. The linearization of (8) can be viewed as the closed-loop dynamics of $\dot{\xi} = J_0 \xi + r_y [1 \ 0 \ \dots \ 0 \ -1]^T u$, $\zeta = [0 \ \dots \ 0 \ 1] \xi$ with (negative) feedback $u = -\hat{h}\zeta$. For given $n > 1$, define $\theta(n) := (\sec(\pi/(n+1)))^{n+1}$, $\hat{h}_d(n) := q + \frac{k_y}{r_y} \frac{\theta(n)}{2+\theta(n)}$, and $\hat{h}_d(1) := q + \frac{k_y}{r_y}$. Then, $J_{\hat{h}}$ is Hurwitz for $q < \hat{h} < \hat{h}_d(n)$ by the secant condition (Thron, 1991; Tyson & Othmer, 1978). If $k_1 = k_2 = \dots = k_n = k_y + r_y(q - \hat{h})$, then $J_{\hat{h}}$ is Hurwitz only if $\hat{h} < \hat{h}_d(n)$. Note that the upper bound $\hat{h}_d(n)$ does not depend on the rate constants k_i of the intermediate reactions. The next proposition establishes another set of bounds.

Proposition 3. Let $\hat{h}_r := q + k_y/(3r_y)$ and $\hat{h}_s := q - k_y/r_y$. If $\hat{h}_s < \hat{h} \leq \hat{h}_r$, then $J_{\hat{h}}$ is Hurwitz for arbitrary values of $n \geq 1$ and k_i . The bounds are tight, i.e., for any value of gain $\hat{h} \notin (\hat{h}_s, \hat{h}_r]$, one can construct an unstable pathway of appropriate size.

4.2. A simple decomposition

Consider the decomposition of the dynamics in (8) into two input–output systems, S_1 and S_2 , governed by

$$S_1 \begin{cases} \dot{x}_1 = z - g_1(x_1) \\ \dot{x}_i = g_{i-1}(x_{i-1}) - g_i(x_i), \quad \text{for } i = 2, \dots, n \\ w = g_n(x_n) \end{cases} \quad (9)$$

$$S_2 \begin{cases} \dot{y} = 2w - f(y) - g_y(y) \\ z = f(y), \end{cases} \quad (10)$$

and interconnected as in Fig. 5. S_1 and S_2 are single-input–single-output systems with n and 1 states, respectively. S_1 is composed of a chain of reactions, and this special structure and the monotonicity of rates g_i make it easier to establish its input–output properties for even large values of n . On the other hand, S_2 includes the “most dominant” nonlinearity in f , due to the dynamics of y and its involvement in autocatalysis and negative feedback. This decomposition separates the complexity of high-dimensional state space of S_1 from that of the important nonlinearity due to autocatalysis isolated in S_2 .

Topcu, Packard, Seiler, and Balas (2009) proposes a method for computing invariant subsets of the RoA for systems with unmodeled dynamics based on certain dissipation inequalities. We apply this idea to the feedback interconnection of S_1 and S_2 to compute invariant subsets of the RoA for (8). For notational simplicity, we rewrite (9) and (10), respectively, as $\dot{x} = F_1(x, z)$, $w = G_1(x)$, and $\dot{y} = F_2(y, w)$, $z = G_2(y)$. Note that $F_1(0, 0) = F_2(0, 0) = G_1(0) = G_2(0) = 0$.

Proposition 4. Let $\delta, \kappa \geq 0$, $U_1 : \mathbb{R}^n \rightarrow \mathbb{R}$ be continuously differentiable, and satisfy $U_1(0) = 0$, $U_1(x) > 0$ for all $x \neq 0$ and

$$\nabla U_1(x) \cdot F_1(x, z) \leq z^2 + 2\delta wz - \kappa w^2, \quad \forall (x, z) \in \mathbb{R}^n \times \mathbb{R}. \quad (11)$$

Let $\mathcal{N}_0 \subseteq \mathbb{R}$ be a (bounded) neighborhood of the origin and $U_2 : \mathbb{R} \rightarrow \mathbb{R}$ be continuously differentiable and satisfy $U_2(0) = 0$, $U_2(y) > 0$ for all $y \neq 0$, and

$$\nabla U_2(y) \cdot F_2(y, w) \leq \kappa w^2 - 2\delta wz - z^2, \quad \forall (y, w) \in \mathcal{N}_0 \times \mathbb{R}. \quad (12)$$

Let $U(x, y) := U_1(x) + U_2(y)$ and α be such that

$$\Omega_{U, \alpha} \subset \mathbb{R}^n \times \mathcal{N}_0. \quad (13)$$

Then, $\Omega_{U, \alpha}$ is invariant under the flow of (8). Furthermore, if one of the inequalities (11) and (12) is strict (except at the origin) then $\Omega_{U, \alpha}$ is a subset of the RoA of the origin for (8).

Proof. Note that $U(0, 0) = 0$, $U(x, y) > 0$ for all nonzero $(x, y) \in \mathbb{R}^{n+1}$, and for all nonzero $(x, y) \in \Omega_{U, \alpha}$, it holds that $\dot{U}(x, y) = \nabla U_1(x) \cdot F_1(x, G_2(y)) + \nabla U_2(y) \cdot F_2(y, G_1(x)) \leq 0$. Hence, $\Omega_{U, \alpha}$ is invariant. If (11) is strict, then $\Gamma_1 := \{(x, y) : \dot{U}(x, y) = 0\} \subset \{(x, y) : x = 0\}$. For all (x, y) with $x = 0$ and $y \neq 0$, it follows that $\dot{x}_1 = f(y)$, $\dot{y} = -f(y) - g_y(y)$, and $g_y(y) \neq 0$ for $y \neq 0$. Consequently, the largest invariant subset of Γ_1 is the origin, and $\Omega_{U, \alpha}$ is a subset of the RoA (by LaSalle’s invariance principle). If (12) is strict, then $\Gamma_2 := \{(x, y) : \dot{U}(x, y) = 0\} \subset \{(x, y) : y = 0\}$. Let $\Gamma_{inv} \subset \{(x, y) : y = 0\}$ be invariant. For $(x, y) \in \Gamma_{inv}$, $\dot{y} = 2g_n(x_n) \neq 0$ for $x_n \neq 0$, which implies that $x_n = 0$. For $(x, y) \in \Gamma_{inv}$, $\dot{x}_n = g_{n-1}(x_{n-1}) \neq 0$ for $x_{n-1} \neq 0$, which implies that $x_{n-1} = 0$. Similarly, for $(x, y) \in \Gamma_{inv}$, it follows that $x_i = 0$ for $i = 1, \dots, n$. Consequently, the largest invariant subset of Γ_2 is the origin, and the result follows by LaSalle’s invariance principle. \square

Proposition 4 constructs RoA certificates for the overall system (8) based on the certificates for the input–output properties of the subsystems S_1 and S_2 established using the dissipation inequalities in (11) and (12), respectively. The quadratic map $z^2 + 2\delta wz - \kappa w^2$ in (11) is called a supply rate for S_1 (similarly its negative is used as a supply rate in (12) for S_2). One diversion from the classical dissipation inequalities literature (Willems, 1972) is that the inequality in (12) is local, i.e., it is supposed to hold in certain bounded subsets (such as certain sublevel sets of associated storage functions) of the state space but not necessarily the whole state space (Topcu, Packard, Seiler et al., 2009). Using special forms of the inequalities (11) and (12), we show that, for specific ranges of \hat{h} , a diagonal function U and α that satisfy the conditions in Proposition 4 (i.e., consequently, $\Omega_{U, \alpha}$ is an invariant subset of the RoA) can be analytically constructed.

4.3. RoA estimation via a local small-gain condition

Let $\delta = 0$, $\kappa = 1$, and (12) hold strictly, i.e.,

$$\nabla U_1(x) \cdot F_1(x, z) \leq z^2 - w^2, \quad \forall (x, z) \in \mathbb{R}^n \times \mathbb{R} \quad (14)$$

$$\nabla U_2(y) \cdot F_2(y, w) < w^2 - z^2, \quad \forall (y, w) \in (\mathcal{N}_0 \setminus \{0\}) \times \mathbb{R}. \quad (15)$$

Lemma 5. The function $U_1 : \mathbb{R}^n \rightarrow \mathbb{R}$, $U_1(x) := \sum_{i=1}^n 2 \int_0^{x_i} g_i(\xi) d\xi$, is continuously differentiable and satisfies $U_1(0) = 0$, $U_1(x) > 0$ for all $x \neq 0$, and (14).

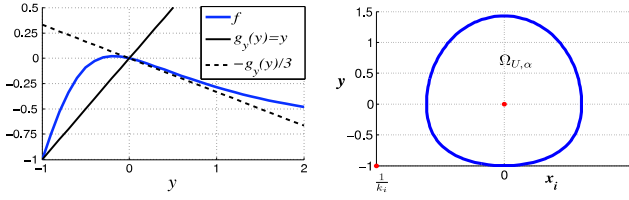


Fig. 6. Left: \mathcal{N}_0 can be constructed as the set of points y where the graph of f lies between g_y and $-\frac{1}{3}g_y$. Right: The $y - x_i$ slice of the invariant subset $\Omega_{U,\alpha}$ with $x_j = 0$, $j \neq i$.

Lemma 6. If $\hat{h}_s < \hat{h} < \hat{h}_r$, then there exists a nonempty (bounded) neighborhood \mathcal{N}_0 of the origin such that the function $U_2 : \mathbb{R} \rightarrow \mathbb{R}$, $U_2(y) := \frac{1}{2} \int_0^y (f(\xi) + g_y(\xi)) d\xi$, is continuously differentiable and satisfies $U_2(0) = 0$, $U_2(y) > 0$ for all nonzero $y \in \mathcal{N}_0$, and (15).

Proof. Denote the set of points y for which the graph of f lies between the graph of g_y and $-\frac{1}{3}g_y$ by $D_1 := \{y : (g_y(y) - f(y))(f(y) + g_y(y)/3) \geq 0\}$ (Fig. 6 (left)). Since $\frac{\partial f}{\partial y}(0) = r_y(q - \hat{h})$ and $\frac{\partial g_y}{\partial y}(0) = k_y > 0$, $\hat{h} < \hat{h}_r = q + \frac{1}{3} \frac{k_y}{r_y} \Rightarrow -\frac{\partial f}{\partial y}(0) < \frac{1}{3} \frac{\partial g_y}{\partial y}(0)$ and $\hat{h} > \hat{h}_s = q - \frac{k_y}{r_y} \Rightarrow \frac{\partial f}{\partial y}(0) < \frac{\partial g_y}{\partial y}(0)$. Therefore, $(g_y(y) - f(y))(f(y) + g_y(y)/3) \geq 0$ is locally satisfied around $y = 0$, and so there is a nonempty neighborhood of the origin $\mathcal{N}_0 \subset D_1 \cup \{0\}$. Direct calculations show that U_2 satisfies the conditions for this \mathcal{N}_0 . \square

Proposition 7. Let U_1, U_2 , and \mathcal{N}_0 be as in Lemmas 5 and 6 and $U(x, y) = U_1(x) + U_2(y)$. Then, for $\hat{h}_s < \hat{h} < \hat{h}_r$ and for any α such that $\Omega_{U,\alpha} \subset \mathbb{R}^n \times \mathcal{N}_0$, the set $\Omega_{U,\alpha}$ is an invariant subset of the RoA for the origin for (8).

Proposition 7 follows from Proposition 4 and Lemmas 5 and 6. The set \mathcal{N}_0 in Lemma 6 can be constructed as the largest sublevel set of U_2 that is contained in D_1 .

Example 8. Let $g_i(x_i) = k_i x_i$, $g_y(y) = y$, $\gamma = \frac{3}{2}$, $q = 1$, and $h = 2$. Then, $\hat{h} = \frac{6}{5}$, $\hat{h}_r = \frac{4}{3}$, $U_1(x) = k_1 x_1^2 + \dots + k_n x_n^2$, $U_2(y) = \frac{5}{12} \log(5 + 6y + 3y^2) + \frac{1}{4}y^2 - \frac{1}{2}y - \frac{5}{12} \log 5$, $U(x, y) = U_1(x) + U_2(y)$, and $\mathcal{N}_0 = \{y : y > -1\}$. The maximum value of α such that U and α satisfy (13) is $\alpha = 0.3682$. Fig. 6 (right) shows the slice of the invariant subset of RoA $\Omega_{U,\alpha}$ in the $y - x_i$ subspace.

4.4. RoA estimation via another dissipation inequality

Consider the case $\kappa = 0$ with (12) holding strictly, i.e.,

$$\nabla U_1(x) \cdot F_1(x, z) \leq z^2 + 2\delta wz, \quad \forall (x, z) \in \mathbb{R}^n \times \mathbb{R} \quad (16)$$

$$\nabla U_2(y) \cdot F_2(y, w) < -z^2 - 2\delta wz, \quad \forall (y, w) \in (\mathcal{N}_0 \setminus \{0\}) \times \mathbb{R}. \quad (17)$$

Lemma 9. For $n > 1$ and $0 < \delta \leq \frac{1}{2}\theta(n)$, there exist positive real numbers d_1, \dots, d_n such that the function $U_1(x) := \sum_{i=1}^n d_i \int_0^{x_i} g_i(\xi) d\xi$ satisfies (16).

Proof. For $n > 1$ and $0 < \delta \leq \frac{1}{2}\theta(n)$, consider the system

$$\begin{aligned} \dot{x}_1 &= -\tilde{z} - g_1(x_1) \\ \dot{x}_i &= g_{i-1}(x_{i-1}) - g_i(x_i), \quad \text{for } i = 2, \dots, n \\ \dot{\tilde{z}} &= 2\delta g_n(x_n) - \tilde{z}, \end{aligned} \quad (18)$$

and let $\tilde{F}(x, \tilde{z})$ denote the vector field in (18). Since $\lim_{|x_i| \rightarrow \infty} \int_0^{x_i} g_i(\xi) d\xi = \infty$, there exist constants $d_1, \dots, d_{n+1} > 0$ so that $\tilde{U}_1(x, \tilde{z}) = \sum_{i=1}^n d_i \int_0^{x_i} g_i(\xi) d\xi + d_{n+1} \frac{1}{2} \tilde{z}^2 = U_1(x) + d_{n+1} \frac{1}{2} \tilde{z}^2$ satisfies $\nabla \tilde{U}_1(x, \tilde{z}) \cdot \tilde{F}(x, \tilde{z}) < 0$ for all nonzero (x, \tilde{z}) (see Corollary 3 in Arcak & Sontag, 2006). Without loss of generality, take $d_{n+1} = 1$, and let $z = -\tilde{z}$; then, for all nonzero (x, z) , it follows that

$$0 > \nabla \tilde{U}_1(x, -z) \cdot \tilde{F}(x, -z) = \nabla U_1(x) \cdot F_1(x, z) - z(2\delta g_n(x_n) + z) = \nabla U_1(x) \cdot F_1(x, z) - 2\delta wz - z^2. \text{ By continuity in } \delta, \text{ we get } \nabla U_1(x) \cdot F_1(x, z) \leq 2\delta wz + z^2 \text{ for all } (x, z). \quad \square$$

Lemma 10. For $n > 1$, let $\delta = \theta(n)/2$ and \hat{h} satisfy $q \leq \hat{h} \leq \hat{h}_d(n)$. Then, there exists a nonempty (bounded) neighborhood \mathcal{N}_0 of the origin such that the function $U_2 : \mathbb{R} \rightarrow \mathbb{R}$, defined as $U_2(y) := -\delta \int_0^y f(\xi) d\xi$, is continuously differentiable and satisfies $U_2(0) = 0$, $U_2(y) > 0$ for all nonzero $y \in \mathcal{N}_0$, and (17).

Proof. Define $D_2 := \{y : f(y)(f(y) + \delta/(1+\delta)g_y(y)) \leq 0\}$. Since $\frac{\partial f}{\partial y}(0) = r_y(q - \hat{h})$ and $\frac{\partial g_y}{\partial y}(0) = k_y > 0$, $\hat{h} < \hat{h}_d(n) = q + \frac{k_y}{r_y} \frac{\theta(n)}{2+\theta(n)} \Rightarrow -\frac{\partial f}{\partial y}(0) < \frac{\delta}{1+\delta} \frac{\partial g_y}{\partial y}(0)$ and $\hat{h} > q \Rightarrow \frac{\partial f}{\partial y}(0) < 0$. Therefore, there exists a nonempty neighborhood of the origin $\mathcal{N}_0 \subset D_2 \cup \{0\}$. Direct calculations show that U_2 satisfies the conditions for this \mathcal{N}_0 . \square

In Lemma 10, \mathcal{N}_0 can be constructed as the largest sublevel set of U_2 contained in D_2 . The following is a direct consequence of Proposition 4 and Lemmas 9 and 10.

Proposition 11. Let $n > 1$ and $\delta = \frac{1}{2}\theta(n)$. Let U_1, U_2 , and \mathcal{N}_0 be as in Lemmas 9 and 10 and $U(x, y) = U_1(x) + U_2(y)$. Then, for $0 < \hat{h} < \hat{h}_d(n)$, and for any α such that $\Omega_{U,\alpha} \subset \mathbb{R}^n \times \mathcal{N}_0$, the set $\Omega_{U,\alpha}$ is an invariant subset of the RoA of the origin for (8).

Proposition 3 and the secant condition establish bounds \hat{h}_r and $\hat{h}_d(n)$ on the values of \hat{h} that guarantee stability of the pathway for arbitrary rates (and number in the case of \hat{h}_r) of the intermediate reactions. Propositions 7 and 11 imply that systems with gains that obey these bounds are simple to analyze, i.e., estimates of the RoA can be constructed through compositional analysis. On the other hand, they do not provide any guarantees on how large these estimates are. In general, the size of these subsets will depend on the properties of f and g_y . When g_1, \dots, g_n, g_y are polynomials (e.g., mass-action kinetics) and f is rational, the search for polynomial U_1 and U_2 that satisfy the conditions in Proposition 4 can be formulated as an SOS program through the S-procedure and SOS relaxations. Topcu, Packard, Seiler et al. (2009) proposes a procedure for enlarging the estimate of the RoA while imposing these SOS constraints. Moreover, it may be possible to enlarge the estimate through an automated search for (sub)optimal supply rates, e.g., for suitable choices for δ and κ in Proposition 4, as discussed in Topcu, Packard, and Murray (2009).

4.5. Existence of block-diagonal Lyapunov functions

The decomposition of (8) into S_1 and S_2 provides a convenient way of searching for block-diagonal Lyapunov functions. The next proposition examines the linearizations of S_1 and S_2 and shows that locally, if there is such a Lyapunov function for the linearization of system (8), then we can construct it by computing U_1 and U_2 satisfying (14) and (15), respectively. Let the linearization of S_1 (around the origin) be $\dot{\tilde{x}} = A_1 \tilde{x} + B_1 \tilde{z}$ and $\dot{\tilde{w}} = C_1 \tilde{x}$ and that of S_2 be $\dot{\tilde{y}} = a_2 \tilde{y} + 2\tilde{w}$ and $\dot{\tilde{z}} = -\sigma \tilde{y}$, where $\sigma := -\frac{\partial f}{\partial y}(0) = r_y(\hat{h} - q)$, $a_2 := -k_y + \sigma$. Rewrite the linearization of (8) as

$$\begin{bmatrix} \dot{\tilde{x}} \\ \dot{\tilde{y}} \end{bmatrix} = J_{\tilde{h}} \begin{bmatrix} \tilde{x} \\ \tilde{y} \end{bmatrix} = \begin{bmatrix} A_1 & -\sigma B_1 \\ 2C_1 & a_2 \end{bmatrix} \begin{bmatrix} \tilde{x} \\ \tilde{y} \end{bmatrix}. \quad (19)$$

Proposition 12. If there exist positive-definite matrices $P_1 \in \mathbb{R}^{n \times n}$ and $p_2 \in \mathbb{R}$ such that $J_{\tilde{h}}^T P + P J_{\tilde{h}}$ is negative definite, where $P = \text{diag}(P_1, p_2)$, then the quadratic functions $U_1(\tilde{x}) := -\frac{\sigma^2}{2a_2 p_2} \tilde{x}^T P_1 \tilde{x}$ and $U_2(\tilde{y}) := p_2 \tilde{y}^2$ are continuously differentiable, positive definite, and,

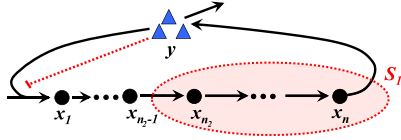


Fig. 7. Illustration of the (n_1, n_2) decomposition of the autocatalytic pathway model in Fig. 1.

for $\delta = \frac{\sigma}{k_y - \sigma}$, satisfy

$$\nabla U_1(\tilde{x}) \cdot (A_1 \tilde{x} + B_1 \tilde{z}) < \tilde{z}^2 + 2\delta \tilde{w} \tilde{z}, \quad \forall (\tilde{x}, \tilde{z}) \in \mathbb{R}^n \times \mathbb{R}, \quad (20)$$

$$\nabla U_2(\tilde{y}) \cdot (a_2 \tilde{y} + 2\tilde{w}) \leq -\tilde{z}^2 - 2\delta \tilde{w} \tilde{z}, \quad \forall (\tilde{y}, \tilde{w}) \in \mathbb{R} \times \mathbb{R}. \quad (21)$$

Lemma 13. For g_1, \dots, g_n such that $\frac{\partial g_i}{\partial x_i}(0) = k$, for $i = 1, \dots, n$, and $\delta > 0$, if there exists a positive-definite matrix P_1 such that $U_1(\tilde{x}) := \tilde{x}^T P_1 \tilde{x}$ satisfies (20), then $\delta < \frac{1}{2}\theta(n)$ and P_1 can be chosen diagonal.

Proposition 14. If $\hat{h} > \hat{h}_d(n)$, $\frac{\partial g_i}{\partial x_i}(0) = k$ for $1 \leq i \leq n$, then there is no quadratic, positive-definite, block-diagonal Lyapunov function of the form $U(\tilde{x}, \tilde{y}) = U_1(\tilde{x}) + U_2(\tilde{y})$ such that $\nabla U(\tilde{x}, \tilde{y}) \cdot J_{\hat{h}}[\tilde{x}^T \tilde{y}^T]^T < 0$ for all nonzero (\tilde{x}, \tilde{y}) .

Proof. Assume, for $\hat{h} > \hat{h}_d(n)$, that there exists a quadratic, block-diagonal function $U(\tilde{x}, \tilde{y}) = U_1(\tilde{x}) + U_2(\tilde{y})$. Then, by Proposition 12, $\delta = \frac{\sigma}{k_y - \sigma}$ and U_1 satisfy (20). On the other hand, Lemma 13 implies that $\delta < \frac{1}{2}\theta(n)$, and the result follows from the contradiction that $\delta = r_y(\hat{h} - q)/(k_y - r_y(\hat{h} - q)) < \theta(n)/2 = r_y(\hat{h}_d - q)/(k_y - r_y(\hat{h}_d - q))$ implies that $\hat{h} < \hat{h}_d(n)$. \square

The partial converse result of Proposition 14 demonstrates a limitation of the analysis based on the decomposition of (8) given in (9) and (10). We next investigate how such limitations may be partially alleviated using more general decompositions of (8).

5. General decomposition

Consider that the system in (8) is decomposed into two input–output systems S_1 and S_2 with n_1 and n_2 states, respectively, as in Fig. 5, where $n_1 + n_2 = n + 1$. Let S_1 and S_2 , respectively, be governed by

$$\dot{\zeta} = \tilde{F}_1(\zeta) + \tilde{B}_1 z, \quad w = \tilde{G}_1(\zeta) = g_n(x_n), \quad (22)$$

$$\dot{\psi} = \tilde{F}_2(\psi) + \tilde{B}_2 w, \quad z = \tilde{G}_2(\psi) = g_{n_2-1}(x_{n_2-1}), \quad (23)$$

where $\tilde{B}_1 = [1 \ 0 \ \dots \ 0]^T$, $\tilde{B}_2 = [2 \ 0 \ \dots \ 0]^T$, and the correspondence between the original states x_1, \dots, x_n, y and the new state variables (in (22) and (23)) is $\psi = [y, x_1, \dots, x_{n_2-1}]^T$ and $\zeta = [x_{n_2}, \dots, x_n]^T$. We call any such feedback interconnection of subsystems with n_1 and n_2 states an (n_1, n_2) -decomposition of (8). Fig. 7 illustrates the (n_1, n_2) -decomposition where S_1 corresponds to part of the pathway as marked and S_2 represents the dynamics of the rest of the pathway. A result similar to Proposition 4 holds for (n_1, n_2) -decompositions.

Proposition 15. Let $\rho : \mathbb{R} \times \mathbb{R} \rightarrow \mathbb{R}$. Let $U_1 : \mathbb{R}^{n_1} \rightarrow \mathbb{R}$ be continuously differentiable and satisfy $U_1(0) = 0$, $U_1(\zeta) > 0$ for all $\zeta \neq 0$, and

$$\nabla U_1(\zeta) \cdot (\tilde{F}_1(\zeta) + \tilde{B}_1 z) \leq \rho(w, z), \quad \forall (\zeta, z) \in \mathbb{R}^{n_1} \times \mathbb{R}. \quad (24)$$

Furthermore, let $\mathcal{N}_0 \subseteq \mathbb{R}^{n_2}$ be a (bounded) neighborhood of the origin, $U_2 : \mathbb{R}^{n_2} \rightarrow \mathbb{R}$ be continuously differentiable and satisfy $U_2(0) = 0$, $U_2(\psi) > 0$ for all $\psi \neq 0$, and

$$\nabla U_2(\psi) \cdot (\tilde{F}_2(\psi) + \tilde{B}_2 w) \leq -\rho(w, z), \quad \forall (\psi, w) \in \mathcal{N}_0 \times \mathbb{R}. \quad (25)$$

Define $U : \mathbb{R}^{n+1} \rightarrow \mathbb{R}$ by $U(\zeta, \psi) := U_1(\zeta) + U_2(\psi)$, and let α be such that $\Omega_{U, \alpha} \subseteq \mathbb{R}^n \times \mathcal{N}_0$. Then, $\Omega_{U, \alpha}$ is invariant under the flow of (8). Furthermore, if one of the inequalities (24) and (25) is strict, except at the origin, then $\Omega_{U, \alpha}$ is a subset of the RoA of the origin for (8).

We now focus on a special case where $\frac{\partial g_i}{\partial x_i}(0) = k$ for $i = 1, \dots, n$. For this case, we showed, in the previous section, that, for $\hat{h}_s < \hat{h} < \hat{h}_d(n)$, we can find block-diagonal Lyapunov functions that give an estimate of the RoA. On the other hand, Proposition 14 establishes that for $\hat{h} > \hat{h}_d(n)$ there is no (quadratic) block-diagonal Lyapunov function of the form $U(x, y) = U_1(x) + U_2(y)$ for the linearization of (8), i.e., the $(n, 1)$ -decomposition cannot produce even a local quadratic Lyapunov function for (8). The following example demonstrates that, for systems with $\hat{h} > \hat{h}_d(n)$, Lyapunov functions can be constructed by increasing the number of states of S_2 .

Example 16. Consider the $(1, 2)$ -decomposition of a pathway with $n = 2$ and $g_i(x_i) = kx_i$. For $\kappa > 0$, $\delta = \frac{\kappa-1}{2}$, and $U_1(x_1) = \frac{1}{2}(1 + \kappa)x_1^2$, it follows that $\nabla U_1(x_1) \cdot (z - kx_1) - z^2 - (\kappa - 1)wz + \kappa w^2 = -(z - kx_1)^2 \leq 0$ for all (x, z) . The inequality in (25) boils down to $\nabla U_2(\psi) \cdot (\tilde{F}_2(\zeta) + \tilde{B}_2 w) \leq \kappa w^2 - (\kappa - 1)wz - z^2$. Fig. 8 (left) shows the set of parameters for which this decomposition yields a block-diagonal Lyapunov function for $q = 1$ and $\frac{\partial g_y}{\partial y}(0) = 1$. A similar analysis is repeated for a pathway with $n = 6$, and the effect of increasing values of n_2 in these decompositions is shown in Fig. 8 (middle).

Fig. 8 (right) shows that, as the size of the pathway increases, the size of the stability region (in the parameter space) decreases and the range of feedback gains becomes limited. For a fixed pathway size, as the feedback gains increase, the corresponding systems approach the stability boundary (in the parameter space), requiring decompositions with larger number n_2 of states in S_2 .

When g_1, \dots, g_n, g_y are polynomial and f is rational, the search for the polynomials U_1 and U_2 that satisfy the conditions in Proposition 15 can be formulated as an SOS programming problem. Under these assumptions, the SOS relaxation for (24) leads to a relatively low degree polynomial in $n_1 + 1$ indeterminate variables, while the SOS relaxation for (25) leads to a relatively high degree polynomial in $n_2 + 1$ (indeterminate) variables. Solving the resulting SOS program, instead of the SOS program for the conditions in Lemma 2, leads to a significant reduction in computational complexity. This reduction stems from the fact that the original SOS program in $n + 1 = n_1 + n_2$ variables is replaced by another with two constraints (in addition to other smaller constraints): one in low number of indeterminate variables ($n_2 + 1$) and the other in comparable (to the original SOS program) number of indeterminate variables ($n_1 + 1$) but lower degree of polynomials. It should also be noted that, for increasing values of n_2 , the computational complexity of the SOS program for the conditions in Proposition 15 will mainly be determined by that of the SOS constraints for (25). Consequently, the decomposition in (22) and (23) and the compositional analysis strategy in Proposition 15 lead to two conflicting trends: increasing the state dimension n_2 of S_2 renders an analysis that is potentially less conservative at the expense of higher computational complexity.

6. Discussion

Both experiments on the glycolysis pathway and simulations of most glycolysis models qualitatively show that unstable modes, such as oscillations in ATP concentration, occur under changes in the experimental conditions (e.g., certain enzyme concentrations) and perturbations in the model parameters (e.g., reaction rates). On the other hand, under fixed experimental conditions or a fixed set of parameters, the behavior of the system is robust to initial

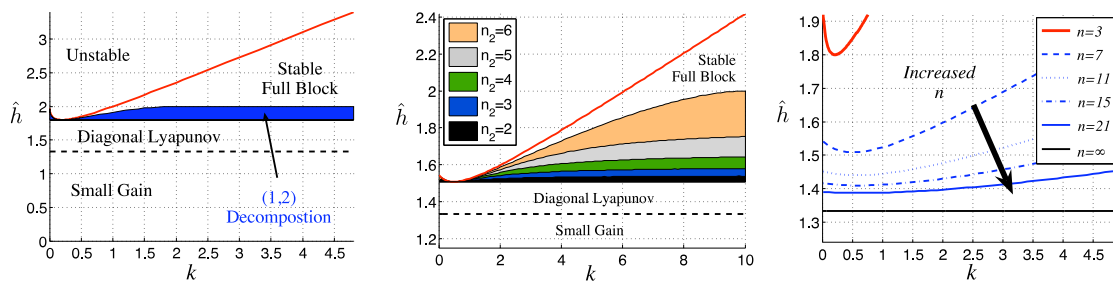


Fig. 8. Left: the (2, 1)-decomposition can only be used to construct Lyapunov functions for the parameter sets labeled by “diagonal Lyapunov” and “small gain”. In addition to these sets, the (1, 2)-decomposition can be used to construct Lyapunov functions for the blue region. Middle: for longer pathways, different (n_1, n_2) -decompositions are used to produce Lyapunov functions that verify subsets of the RoA. For fixed k , as the feedback gain \hat{h} approaches the stability boundary, construction of Lyapunov functions requires larger values of n_2 . The figure illustrates this trend for $n = 6$. Right: as the size of the pathway increases, the size of the stability region (in the parameter space) decreases.

condition perturbations (Dano et al., 2006; Hynne et al., 2001; Nielsen & Sorensen, 1998; Richard, 2003). We have discussed an approach based on system-theoretic measures, such as the extent of the region of attraction (RoA) around the nominal operating points of the system, to prove robustness under perturbations of the initial conditions. We have demonstrated the use of the approach on a specific class of autocatalytic pathway models that capture the core structure of the glycolysis pathway.

We have also shown that the size of the estimated (through a numerical optimization-based procedure) RoA around the nominal operating condition provides information about the robustness of the model to parameter perturbations. More specifically, numerical experiments demonstrated that systems that are robust with respect to perturbations in the parameter space have large, easily “verifiable” (in terms of proof complexity) estimates of the RoA. Additionally, for systems close to the stability boundary, small changes in the value of feedback strength lead to several different regimes in which “simple” polynomial Lyapunov functions (i) certify large invariant subsets of the RoA; (ii) can only certify relatively smaller sets to be in the RoA; and (iii) cannot certify (to the tolerances used in the numerical computations) any invariant subset of the RoA. This optimization-based procedure becomes computationally impractical as the pathway size increases. In order to extend the RoA analysis to larger pathways, we took a compositional approach which exploited a natural decomposition of the system, induced by the underlying biological structure. The pathways were decomposed into a feedback interconnection of two input–output subsystems: a small subsystem with complicating nonlinearities and a large subsystem with simple dynamics. This decomposition simplified the analysis by assembling RoA certificates based on the input–output properties of the subsystems. The simplest decomposition (in Section 4) allowed us to analytically construct, using storage functions and simple quadratic supply rates, block-diagonal Lyapunov functions for a large family of autocatalytic pathways. We showed that if a Lyapunov function of the specified block-diagonal form exists, then it can be constructed using this decomposition. For analysis of a larger class of pathways, more general versions of the decomposition were required, allowing for the size of the subsystem with the complicating nonlinearity to increase. This strategy led to two conflicting trends: a larger family of pathway models become amenable to RoA analysis at the expense of computational complexity.

References

- Alberts, B., Johnson, A., Lewis, J., Raff, M., Roberts, K., & Walter, P. (2002). *Molecular biology of the cell* (4th ed.) Garland.
- Arcak, M., & Sontag, E. D. (2006). Diagonal stability of a class of cyclic systems and its connection with the secant criterion. *Automatica*, 42(9), 1531–1537.

- Arcak, M., & Sontag, E. D. (2008). A passivity-based stability criterion for a class of biochemical reaction networks. *Mathematical Biosciences and Engineering*, 5(1), 1–19.
- Banuelos, M., Gancedo, C., & Gancedo, J. M. (1977). Activation by phosphate of yeast phosphofructokinase. *Journal of Biological Chemistry*, 252(18), 6394–6398.
- Chandra, F. A., Buzi, G., & Doyle, J. C. (2009). Linear control analysis of the autocatalytic glycolysis system. In *Proceedings American control conference* (pp. 319–324).
- Dano, S., Madsen, M. F., Schmidt, H., & Cedersund, G. (2006). Reduction of a biochemical model with preservation of its basic dynamic properties. *FEBS Journal*, 273(21).
- de Leenheer, P., Angeli, D., & Sontag, E. D. (2007). Monotone chemical reaction networks. *Journal of Mathematical Chemistry*, 41(3), 295–314.
- Feinberg, M. (1988). Chemical reaction network structure and the stability of complex isothermal reactors: II multiple steady states for networks of deficiency one. *Chemical Engineering Science*, 43, 1–25.
- Feinberg, M. (1995). The existence and uniqueness of steady states for a class of chemical reaction networks. *Archive for Rational Mechanics and Analysis*, 132, 311–370.
- Horn, F., & Jackson, R. (1972). General mass action kinetics. *Archive for Rational Mechanics and Analysis*, 47(2), 81–116.
- Hynne, F., Dano, S., & Sorensen, P. G. (2001). Full-scale model of glycolysis in *Saccharomyces cerevisiae*. *Biophysical Chemistry*, 94(1–2), 121–163.
- Khalil, H. K. (2002). *Nonlinear systems* (3rd ed.) Prentice Hall.
- Nielsen, K., & Sorensen, P. G. (1998). Sustained oscillations in glycolysis: an experimental and theoretical study of chaotic and complex periodic behavior and quenching of simple oscillations. *Biophysical Chemistry*, 72, 49–62.
- Parrilo, P. (2003). Semidefinite programming relaxations for semialgebraic problems. *Mathematical Programming, Series B*, 96(2), 293–320.
- Richard, P. (2003). The rhythm of yeast. *FEMS Microbiology Reviews*, 27, 547–557.
- Sontag, E. D. (2007). Monotone and near-monotone biochemical networks. *Systems and Synthetic Biology*, 1(2), 59–87.
- Thron, C. D. (1991). The secant condition for instability in biochemical feedback control—parts I and II. *Bulletin of Mathematical Biology*, 53, 383–424.
- Topcu, U., & Packard, A. (2009). Local stability analysis for uncertain nonlinear systems. *IEEE Transactions on Automatic Control*, 54, 1042–1047.
- Topcu, U., Packard, A., & Murray, R. (2009). Compositional stability analysis based on dual decomposition. In *Proceedings conference on decision and control* (pp. 1175–1180).
- Topcu, U., Packard, A., & Seiler, P. (2008). Local stability analysis using simulations and sum-of-squares programming. *Automatica*, 44, 2669–2675.
- Topcu, U., Packard, A., Seiler, P., & Balas, G. (2009). Stability region estimation for systems with unmodeled dynamics. In *Proceedings European control conference*.
- Topcu, U., Packard, A., Seiler, P., & Balas, G. (2010). Help on SOS. *IEEE Control Systems Magazine*, 30, 18–23.
- Tyson, J. J., & Othmer, H. G. (1978). The dynamics of feedback control circuits in biochemical pathways. In R. Rosen, & F. M. Snell (Eds.), *Progress in theoretical biology: Vol. 5* (pp. 1–62). Academic Press.
- Willems, J. C. (1972). Dissipative dynamical systems I: general theory. *Archive for Rational Mechanics and Analysis*, 45, 321–343.



Gentian Buzi is a postdoctoral scholar in Control and Dynamical Systems at the California Institute of Technology. He has a B.S. in Computer Science and Physics, SUNY Fredonia (2000), an M.S. in Electrical Engineering, California Institute of Technology (2002), and a Ph.D. in Control and Dynamical Systems, California Institute of Technology (2010). His research focuses on the underlying principles that govern the behavior of complex systems with an emphasis on systems biology and engineering applications.



Ufuk Topcu is a postdoctoral scholar in Control and Dynamical Systems at the California Institute of Technology. His research focuses on developing analytical and computational tools that aim to systematically and automatically close the specification–design–verification loop for networked dynamical systems. He received his Ph.D. in 2008 from the University of California, Berkeley.



John C. Doyle is the John G. Braun Professor of Control and Dynamical Systems, Electrical Engineer, and BioEngineering at Caltech. He has a B.S. and M.S. in EE, MIT (1977), and a Ph.D., Math., UC Berkeley (1984). Current research interests are in theoretical foundations for complex networks in engineering and biology, focusing on architecture, and for multiscale physics. Early work was in the mathematics of robust control, including LQG robustness, (structured) singular value analysis, H -infinity, plus recent extensions to nonlinear and hybrid systems. His research group has collaborated in many software projects, including the Robust

Control Toolbox (μ Tools), SOSTOOLS, SBML (Systems Biology Markup Language), and FAST (Fast AQM, Scalable TCP). Prize paper awards include the IEEE Baker, the IEEE Automatic Control Transactions Axelby (twice), and best conference papers in ACM Sigcomm and AACC American Control Conference. Individual awards include the AACC Eckman, and the IEEE Control Systems Field and Centennial Outstanding Young Engineer Awards. He has held national and world records and championships in various sports.